COBEM2015

ABCM Associação Brasileira de Engenharia e Ciências Mecânicas

23rd ABCM International Congress of Mechanical Engineering
December 6-11, 2015, Rio de Janeiro, RJ, Brazil

A NOVEL ONE-DIMENSIONAL CONSTITUTIVE MODEL FOR SHAPE MEMORY ALLOYS

Achille A. Bassi
Marcelo A. Savi
Universidade Federal do Rio de Janeiro
COPPE - Departamento de Engenharia Mecânica
Centro de Mecânica Não-Linear
Caixa Postal 68.503, 21945-970 - Rio de Janeiro - Brasil
arantesb@hotmail.com
savi@mecanica.coppe.ufrj.br

Abstract. *This paper presents a novel constitutive model to describe the thermomechanical behavior of shape memory alloys (SMAs). The proposed model is developed within the scope of the standard generalized material formalism. Inelastic behavior includes both phase transformation and classical plasticity. Solid phase transformations are described considering four macroscopic phases representing three variants of martensite and an austenitic phase. Classical plasticity is described considering both kinematic and isotropic hardening. Under these assumptions, the proposed model can fit threshold stress-strain-temperature curves from the transformation surfaces representing multiple simultaneous phase transformation processes. Numerical simulations are carried out establishing a comparison with experimental data available in literature.*

Keywords: *Shape Memory Alloys, Constitutive Model, Shape Memory Effect, Pseudoelasticity*

1. INTRODUCTION

Shape memory alloys (SMAs) belong to the smart materials presenting a complex thermomechanical behavior due to solid-phase transformations. Several behaviors can be observed under themomechanical loadings and it is important to highlight: Shape Memory Effect (SME) that represents the capability to recover residual inelastic strains after a proper themomechanical loading; Pseudoelasticity (PE) that is related to the capability of recover large strains through an inelastic hysteretic mechanical cycle. Due to these unique properties, SMAs have several applications on engineering, medicine, dentistry, and other potential areas. They can be used in a passive way, as structural elements, or in a active way, as actuators and sensors. Among their applications, it should be pointed out absorption of vibration or impact; high pressure pipe couplings; self-expanding structures; and adaptive structures. A general overview of the SMAs' applications can be found in Lagoudas (2008).

The development of an SMA application has the special need of a proper mathematical description for each phenomenon involved. Nevertheless, the nonlinear thermomechanical behaviors make this task a special challenge, involving several research efforts. According Lagoudas (2008), although the SME has had first reported in 1963, the first constitutive models are associated with 1980's. In general, SMA description is performed by considering three different approaches: macroscopic - based on the continuum mechanics; microscopic - based on the interaction among the crystals and grains, or micro-planes; mesoscopic - that considers the macroscopic field from some microscopic effects as variations of volume fractions of the phases Bo and Lagoudas (1999).

Lagoudas (2008) and Paiva and Savi (2006) presented general overviews about constitutive models for SMAs. de Souza (1998) stated a model based on the generalized standard formalism, with a Helmholtz free energy function having constant coefficients, and dissipation functions adapted from the classical plasticity theory. That model was built for 3D media and has drag and deviatoric components. Three different criteria for phase transformation, each one based on distinct elasticity criterion, are adapted from the Drucker-Prager flux. This model needs to set a parent phase and does not represent changes in properties of austenitic and martensitic phases.

Auricchio and co-workers developed a model using the generalized plasticity theory to represent stress induced martensite. Parallel surfaces for direct and reverse transformations are considered without any hardening function. Under these assumptions, the model has the same properties for martensite and austenite and the description of SME is restrict to the gap between the transformation surfaces.

Paiva *et al.* (2005) proposed a one-dimensional model that follows the same ideas of Savi *et al.* (2002). This model proposed energy functions based on the mixture of four macroscopic phases (austenite, twinned martensite, tensile martensite and compressive martensite). The generalized standard material formalism was employed using indicator functions

to establish restrictions on volume fractions mixture. A large number of behaviors can be described by this model as SME, PE, internal subloops due to incomplete phase transformations, two-way shape memory effect (TWSME) and tension-compression asymmetry. In addition, the model has viscous behavior that allows the representation of thermo-mechanical couplings. Its current version includes phenomena like transformation induced plasticity effect (TRIP) for three-dimensional medias.

Bo and Lagoudas (1999) proposed a one-dimensional constitutive model based on the Gibbs free energy with a parent phase transforming in a product phase through relations based on the classical theory of plasticity. The current state of the Lagoudas' familiy proposed an extension of the original model for three-dimensional media, including three macroscopic phases (seff accommodated martensite, detwinned martensite and austenite). This model employed different hardening rules and a wide set of phenomena can be described (SME, TWSME, PE, TRIP and internal subloops). This model presents a constant thermodynamic resistance to the phase transformation that results in parallel transformation surfaces. Moreover, it does not allow the description of compressive behavior since it does not use a compressive martensitic variant.

Rizzoni and Marfia (2015) stated a unified model derived from Hemlmoltz free energy with Voight mixture and Gibbs free energy with Reuss homogenization, restriction rules on the phase diagram and three microscopic phases (austenite, compressive and tensile martensites). Twinned martensite is treated as a mixture from the detwinned variants. Phase transformations are defined from parallel surfaces. Numerical simulations were conducted for isothermal processes.

This paper deals with a novel SMA constitutive model. The idea is to characterize inelastic behavior from the definition of phase transformation and plastic surfaces. Four macroscopic phases are considered. The model is developed within the scope of the generalized standard material formalism and continuum mechanics. A Helmholtz free energy function of the SMA results from a combination of the energy functions for each of its four macroscopic phases. As in many of the model for SMAs, theory of plasticity is used as an inspiration for the definition of the inelastic behavior resulting either from yield or phase transformation surfaces. Phase tranformation surfaces has nonparallel representation as observed on experimental data. Classical plasticity description considers both isotropic and kinematic hardening. In addition, the model presents a plastic-phase transformation coupling. A critical analysis of this new model can consider it as a combination of the main ideas of de Souza (1998) and Auricchio *et al.* (1997) together with those proposed by Paiva *et al.* (2005). The resulting model is close to the proposed by Bo and Lagoudas (1999). For the sake of simplicity, TRIP, internal subloops, TWSME are not treated in this paper.

2. CONSTITUTIVE MODEL

In brief the generalized standard material approach relies in the definition of two potentials from which the associated variables and flux variables are derived.

The first potential is the free energy $\Psi(\varepsilon, T, \mathbf{V})$, where ε and T are the observable variables and $\mathbf{V}$ is the internal variables set. Stress and entropy can be related to this potential through the equations (1) and (2), and it is used to define the thermodynamic forces, or associated variables to the internal variables, Eq. (3). The strain is additively partitioned in elastic and inelastic components $\varepsilon = \varepsilon_e + \varepsilon_{in}$.

$$\sigma = \rho\frac{\partial\Psi}{\partial\varepsilon_e} = \rho\frac{\partial\Psi}{\partial\varepsilon} = -\rho\frac{\partial\Psi}{\partial\varepsilon_{in}} \tag{1}$$

$$s = -\frac{\partial\Psi}{\partial T} \tag{2}$$

$$A_{V_i} = -\rho\frac{\partial\Psi}{\partial V_i} \tag{3}$$

The second potential, the intrinsic dissipation[1], is a convex scalar field, function of the flux variables (internal variables time rates), related to the dissipative processes. Herein the conjugated dissipation, function of the thermodynamic forces, is being used instead. This conjugated scalar field can be derived from the former one by the Legendre-Fenchel transform, Eq. (4), and the result is a null scalar field inside the phase diagram's elastic areas, Eq. (5).

$$\Phi_I^*(\dot{V}^*) = \underset{\dot{V}}{sup}\{\dot{V}^* \cdot \dot{V} - \Phi_I(\dot{V})\} = \sup_{\dot{V}}\left\{\left(\dot{V}^* - A_V\right)\dot{V}\right\} \tag{4}$$

$$\Phi_I^* = \begin{cases} 0 & \text{, if } f < 0 \\ \text{undefined} & \text{, if some } f = 0 \text{ and } \dot{\mathbf{V}} \neq \underline{0} \\ +\infty & \text{otherwise} \end{cases} \tag{5}$$

[1] Just dissipation from now on

Since Φ_I^* is not differentiable when $\dot{V}^* = A_V$, then $\dot{V} \in \partial_{\dot{\mathbf{V}}^*}\phi^*$ when the flux variable is not zero. So the solution for the flux variables comes from the maximum dissipation principle, that establishes that the dissipation is the maximum kinematically feasible value that respects internal variables restrictions. Using Lagrange's multipliers, it is possible to write the Eq. (6), so each flux variable can be purchased by the Eq. (7).

$$\chi = \max\{\phi_I^*(\dot{\mathbf{V}}^*) - \dot{\lambda} f(\dot{\mathbf{V}}^*)\} \tag{6}$$

$$\frac{\partial \chi}{\partial \dot{V}_i^*} = 0 \tag{7}$$

These equations allow one to write the flux variables as functions of the Lagrange's multipliers, $\dot{\lambda}_i$, which need to be calculated from the Kuhn-Tucker conditions: $\dot{f}_j \dot{\lambda}_j = 0$, $f_j \dot{\lambda}_j = 0$, $f_j \leq 0$ and $\dot{\lambda}_i \geq 0$. Based on that, the following evolution law is defined:

$$\dot{V}_i = \sum_{j=1}^{NRest} \left(\dot{\lambda}_j \frac{\partial f_j}{\partial \dot{V}_i^*} \right) \tag{8}$$

2.1 SMA model

This section presents the SMA model employing the formalism presented in the previous section. Free energy density is initially presented. Afterward, potential of dissipation is presented defining inelastic phenomena: phase transformation and yield surfaces.

2.1.1 Free Energy Potential

A Helmholtz free energy function is proposed for each macroscopic phase: austenite, twinned martensite, positive and negative detwinned martensite.

$$M^+: \quad \rho\Psi_1(\varepsilon, T) = \tfrac{_ME}{2}\varepsilon^2 - \tfrac{^T}{_M}H(T - T_0)\varepsilon + \Lambda_1 \tag{9}$$

$$M^-: \quad \rho\Psi_2(\varepsilon, T) = \tfrac{_ME}{2}\varepsilon^2 - \tfrac{^T}{_M}H(T - T_0)\varepsilon + \Lambda_2 \tag{10}$$

$$A: \quad \rho\Psi_3(\varepsilon, T) = \tfrac{_AE}{2}\varepsilon^2 - \tfrac{^T}{_A}H(T - T_0)\varepsilon + \Lambda_3 \tag{11}$$

$$M: \quad \rho\Psi_4(\varepsilon, T) = \tfrac{_ME}{2}\varepsilon^2 - \tfrac{^T}{_M}H(T - T_0)\varepsilon + \Lambda_4 \tag{12}$$

Considering the the same specific weight to all phases, and Λ_i as the sum of a enthalpy and a specific heat, Eq (13), a global free energy function for the mixture can be stated by using the phases' volumetric fractions, β_k, a phase interaction term, P_{Int}, and a restriction for phase coexistence. This constrain was imposed by a indicator function, $I_{\mathbb{B}}(\underline{\beta})$, which is defined by the property in the Eq. (15), for the group stated in the Eq. (16).

$$\Lambda_i = {}_0\Lambda_i + {}_T\Lambda_i T \tag{13}$$

$$\rho\overline{\Psi}(\varepsilon, T, \underline{\beta}) = \sum_{i=1}^{4} [\beta_i \Psi_i(\varepsilon, T)] + P_{Int}(\underline{\beta}) + I_{\mathbb{B}}(\underline{\beta}) \tag{14}$$

$$I_{\mathbb{B}}(\underline{\beta}) = \begin{cases} 0 & \text{, if } \underline{\beta} \in \mathbb{B} \\ +\infty & \text{, otherwise} \end{cases} \tag{15}$$

$$\mathbb{B} = \left\{ \beta_i \in \mathbb{R} \,/\, \sum_{i=1}^{4} \beta_i = 1 \text{ and } 0 \leq \beta_i \leq 1 \right\} \tag{16}$$

In order to establish a comparison with the preceding section, the following vectors are defined:

$$\underline{V} = [\varepsilon_\beta \; \beta_1 \; \beta_2 \; \beta_3 \; \beta_4 \; \varepsilon_p \; \alpha_I \; \alpha_K]^t \tag{17}$$

$$\underline{v} = [\beta_1 \; \beta_2 \; \beta_3 \; \beta_4 \; \alpha_I \; \alpha_K]^t \tag{18}$$

$$\underline{A}_V = \left[A_{\varepsilon_\beta} \; A_{\beta_1} \; A_{\beta_2} \; A_{\beta_3} \; A_{\beta_4} \; A_{\varepsilon_p} \; A_{\alpha_I} \; A_{\alpha_K}\right]^t \tag{19}$$

Under these assumptions, the free energy from the Eq. (14) can receive classical plasticity with linear isotropic and kinematic hardenings whose coefficients where arbitrated to follow the Voigt mixture law, Eq. (22), the same rule derived for the other coefficients present in each Ψ_i, E and ${}^{T}H$.

$$\rho\Psi(\varepsilon,\underline{V}) = \frac{E}{2}(\varepsilon_e)^2 - {}^{T}H(T-T_0)(\varepsilon_e) + \underline{\beta}\cdot\underline{\Lambda} + \frac{1}{2}\underline{v}^t\, diag(H_{\beta_1},H_{\beta_2},H_{\beta_3},H_{\beta_4},H_I,H_K)\underline{v} + I_{\mathbb{B}}(\underline{\beta}) \tag{20}$$

$$\varepsilon_e = \varepsilon - \varepsilon_\beta - \varepsilon_p \tag{21}$$

$$[] = {}_{M}[] + \beta_3({}_{A}[] - {}_{M}[]) \tag{22}$$

2.1.2 Inelastic surfaces

Irreversible processes are described with the aid of the pseudo-potential of dissipation. Essentially, irrerversibilities are associated with inelastic behavior, here represented by phase transformations and plasticity. These behaviors are defined by inelastic surfaces and, inside these surfaces, only reversible, elastic processes occur. The definition of the phase transformations surfaces are based on the phase diagram shown in the Fig. (1). All possibilities are represented in other surfaces shown in the Fig. 2. Note that each transformation is defined by the start and the finish surfaces. On the other hand, plastic inelastic behavior is defined from classical yield surfaces.

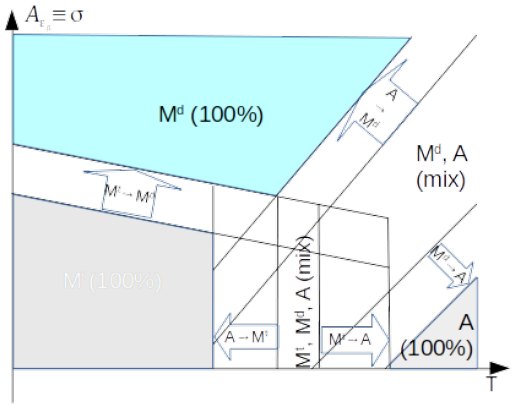

Figure 1: Glimpse of a phase diagram for a generic SMA proposed by Lagoudas (2008, Fig 6.4)

Although any kind of function can be employed to approximate the phase transformation surfaces, due the simplicity and to agree with the reference models, linear functions are adopted. In brief, the model's pseudo-potential of dissipation is defined as a sum of the individual dissipations due to each of the inelastic processes, all elastic criteria were arranged in the vector f. Concerning phase transformation, the function $F_{i\,j}$ defines the transformation surface from phase i to phase j. Hence, during a thermomechanical process, $F_{i\,j} < 0$ implies there is no dissipation due to the mechanism $i\,j$. Besides, defining F_p is the yield surface. These restrictions are taken from the linear Drucker-Prager flux. It is also possible to employ smooth functions using different potentials, derived from different hardening functions.

$$f = \begin{bmatrix} F_{1\,2} \\ F_{2\,1} \\ F_{1\,3} \\ F_{3\,1} \\ F_{4\,1} \\ F_{2\,3} \\ F_{3\,2} \\ F_{4\,2} \\ F_{3\,4} \\ F_{4\,3} \\ F_p \end{bmatrix} = \begin{bmatrix} -A_{\varepsilon_\beta} + (A_{\beta_2} - A_{\beta_1})/e_{1\,2} + ({}^{0}K_{1\,2} + {}^{T}K_{1\,2}T) \\ A_{\varepsilon_\beta} + (A_{\beta_1} - A_{\beta_2})/e_{1\,2} - ({}^{0}K_{2\,1} + {}^{T}K_{2\,1}T) \\ -A_{\varepsilon_\beta} + (A_{\beta_3} - A_{\beta_1})/e_{1\,3} + ({}^{0}K_{1\,3} + {}^{T}K_{1\,3}T) \\ A_{\varepsilon_\beta} + (A_{\beta_1} - A_{\beta_3})/e_{1\,3} - ({}^{0}K_{3\,1} + {}^{T}K_{3\,1}T) \\ A_{\varepsilon_\beta} + (A_{\beta_1} - A_{\beta_4})/e_{1\,4} - ({}^{0}K_{4\,1} + {}^{T}K_{4\,1}T) \\ A_{\varepsilon_\beta} + (A_{\beta_3} - A_{\beta_2})/e_{2\,3} - ({}^{0}K_{2\,3} + {}^{T}K_{2\,3}T) \\ -A_{\varepsilon_\beta} + (A_{\beta_2} - A_{\beta_3})/e_{2\,3} + ({}^{0}K_{3\,2} + {}^{T}K_{3\,2}T) \\ -A_{\varepsilon_\beta} + (A_{\beta_4} - A_{\beta_2})/e_{2\,4} + ({}^{0}K_{4\,2} + {}^{T}K_{4\,2}T) \\ A_{\beta_4} - A_{\beta_3} - K_{3\,4} \\ A_{\beta_3} - A_{\beta_4} - K_{4\,3} \\ |A_{\varepsilon_p} + A_{\alpha_K}| - (\sigma_y - A_{\alpha_I}) \end{bmatrix} \tag{23}$$

The evolution of internal variables is calculated applying the Eq. (8) to the restrictions in the Eq. (23).

3. MODEL PARAMETERS

The proposed model has several parameters summarized in Tab. 1. They have to be adjusted in order to make the model fit each specific material being modeled.

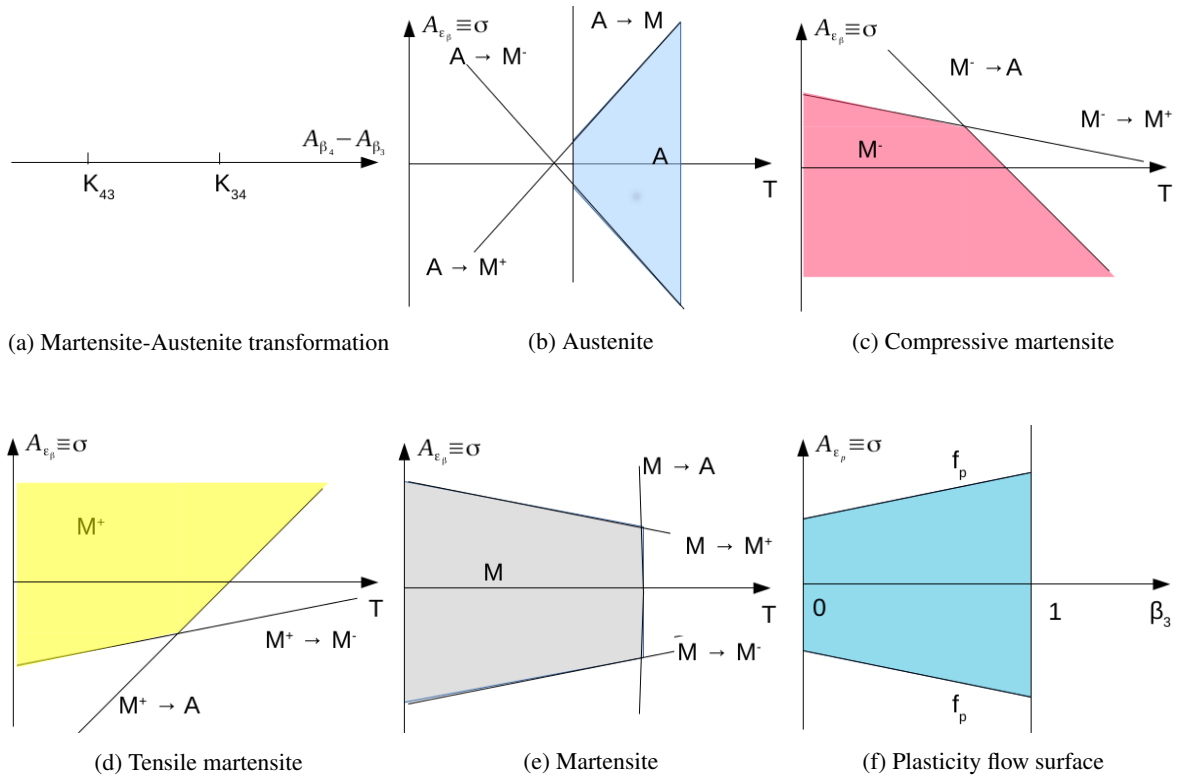

(a) Martensite-Austenite transformation (b) Austenite (c) Compressive martensite

(d) Tensile martensite (e) Martensite (f) Plasticity flow surface

Figure 2: Transformation surfaces

Table 1: **Model Parameters**

SYMBOL	PHYSICAL INTERPRETATION
E_A	Austeninic/martensitic phase elasticity modulus
E_M	
${}^T_A H$	Austenitic/martensitic phase thermal stress modulus
${}^T_M H$	
${}_A H_I$	Austeninic/martensitic phase isotropic hardening
${}_M H_I$	
${}_A H_K$	Austeninic/martensitic phase kinematic hardening
${}_M H_K$	
${}_A \sigma_y$	Austeninic/martensitic phase yielding stress
${}_M \sigma_y$	
${}_i \Lambda_0$	Phase formation enthalpy
${}_i \Lambda_T$	Phase specific heat
${}^0 K_{i\,j}$	Linear approximation coefficients for the material's resistance to transform from the phase i to j
${}^T K_{i\,j}$	
H_{β_i}	Phase transformation kinetics characteristics defining the slope of the plateau involving β_i changes
$e_{i\,j}$	The transformation strain in transformation between the phases i and j
$K_{3\,4}$	Material's resistances to transform from the phases 3 to 4 and the reversal
$K_{4\,3}$	

4. NUMERICAL SIMULATIONS

In order to calculate the internal variables' evolution it was implemented a implicit Euler scheme, Eq. (25). All loads were applied with imposed stress and temperature states, so the thermal evolution aspects could be neglected and the strain state resulted from the model.

$$t^{(k+1)} = t^{(k)} + \Delta_t k,\ k \in \mathbb{N}_+^* \tag{24}$$

$$\underline{V}^{(k+1)} = \underline{V}^{(k)} + \dot{\underline{V}}^{(k+1)} \Delta_t \tag{25}$$

The model verification was performed by considering experimental data from Tobushi *et al.* (1991). Tensile behavior was adopted as the reference and all parameter estimation is done considering the experimental curves of Tobushi *et al.* (1991, Figures 3, 6 and 9). As there is no classical plasticity within the Tobushi *et al.* (1991)'s results, all plastic parameters were adjusted to be in the expected place in the stress-strain space, which was inspired by the from Lagoudas (2008, Fig. 6.4), and they were arbitrarily chosen close to Lagoudas (2008, Tab 2.5). The table 2[2] shows the model parameters used to generate the results, which include parameters chosen to show the model capabilities related to subjects not present in the reference paper.

Table 2: Model's parameters for Tobushi *et al.* (1991)

E_A $3.758E+10$	${}^{T}_{A}H$ $2.612E+06$	${}_{A}H_K$ $2.000E+09$	${}_{A}H_I$ $2.000E+09$	${}_{A}S_y$ $7.000E+08$	E_M $2.429E+10$	${}^{T}_{M}H$ $1.668E+06$
${}_{M}H_I$ $1.500E+09$	${}_{M}H_K$ $1.500E+09$	${}_{M}S_y$ $6.500E+08$	${}_{3}\Lambda_T$ $-1.878E+05$	${}_{4}\Lambda_0$ $0.000E+00$	${}_{4}\Lambda_T$ $0.000E+00$	H_{β_1} $3.625E+05$
H_{β_2} $3.625E+05$	H_{β_3} $3.393E+06$	H_{β_4} $3.625E+05$	${}^{0}K_{1\,2}$ $-1.240E+08$	${}^{T}K_{1\,2}$ $0.000E+00$	${}^{0}K_{2\,1}$ $2.440E+08$	${}^{T}K_{2\,1}$ $-5.000E+05$
${}^{0}K_{1\,3}$ $-3.343E+09$	${}^{T}K_{1\,3}$ $6.473E+06$	${}^{0}K_{3\,1}$ $-1.194E+09$	${}^{T}K_{3\,1}$ $9.642E+05$	${}^{0}K_{4\,1}$ $1.881E+08$	${}^{T}K_{4\,1}$ $-3.333E+05$	${}^{0}K_{2\,3}$ $3.445E+09$
${}^{T}K_{2\,3}$ $-5.971E+06$	${}^{0}K_{3\,2}$ $1.159E+09$	${}^{T}K_{3\,2}$ $-1.402E+05$	${}^{0}K_{4\,2}$ $-1.224E+08$	${}_{T}K_{4\,2}$ $0.000E+00$	${}^{0}K_{3\,4}$ $-5.294E+07$	${}^{0}K_{4\,3}$ $6.045E+07$
$e_{1\,2}$ $9.600E-02$	$e_{1\,3}$ $5.300E-02$	$e_{1\,4}$ $5.300E-02$	$e_{2\,3}$ $4.300E-02$	$e_{2\,4}$ $4.300E-02$		

4.1 Model Verification

Model verification starts considering SME and PE. Isothermal load cycles at three different temperatures are treated. Figure (3) establishes a comparison between numerical and experimental data due to Tobushi *et al.* (1991). Note that the model is able to capture the general thermomechanical behavior of SMAs for different temperatures.

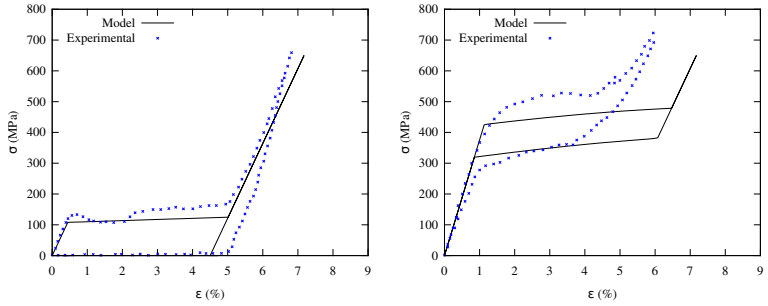

(a) Shape memory cycle (280 K), model against Tobushi *et al.* (1991)

(b) Pseudoelastic cycle (373 K), model against Tobushi *et al.* (1991)

Figure 3: Model response compared to experimental results

4.2 General Simulations

The general model capabilities are now investigated by considering parameters presented in Tab. 2. Initially, isothermal tests for different temperatures are carried out. Figure (4a) shows the stress-strain curves for three different temperatures, starting at austenitic phase and therefore, presenting PE effect. Figure (4b) presents the low temperature behavior,

[2]The missing parameters are null

starting at twinned martensitic phase. Thermal loading is treated in Fig. (4c) showing strain-temperature curves for different, constant, stress levels. Note the hysteretic loops of stress-strain curves change their sizes and shapes according to the temperature level. The same can be said related to hysteresis loop for strain-temperature curves depending on both temperature or stress level.

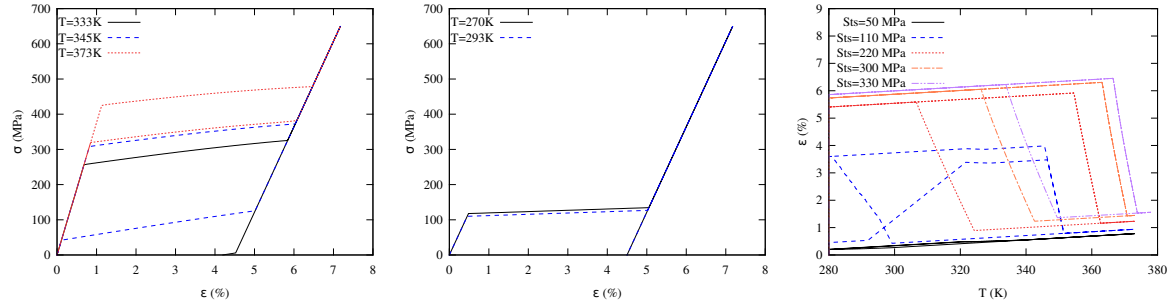

(a) Pseudoelastic tensile cycles for several temperatures (b) Shape memory tensile cycles for several temperatures (c) Thermal cycles for several constant stresses

Figure 4: Model response under different conditions for the parameters in the Tab. 2

Different loadings are now in focus considering both tensile and compressive behaviors. Figure (5) shows the general tension-compression behavior using the parameters of Tab. 2. Note the asymmetric behavior and also the capability of the model to represent the expected behaviors to alternated loads under different temperatures. It is important to highlight the martensitic behavior for low temperatures, which includes detwinning and reorientation ($M^+ \rightarrow M^-$ and $M^- \rightarrow M^+$).

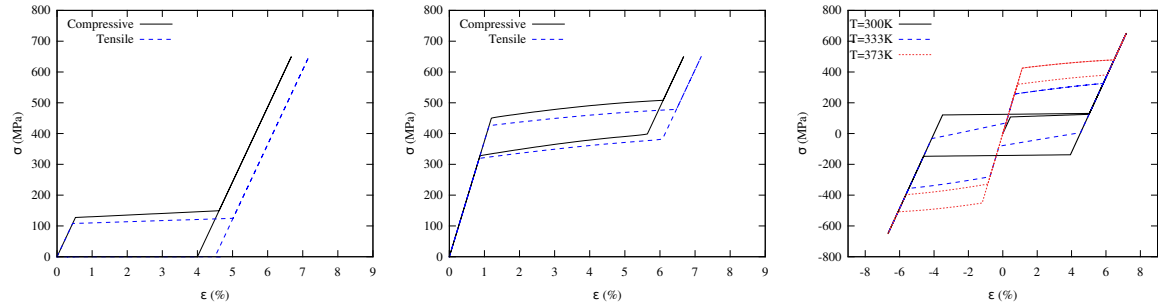

(a) Tensile-compressive asymmetry under SM regime (280 K) (b) Tensile-compressive asymmetry under PE regime (373 K) (c) Alternated tensile-compressive isothermal cycles

Figure 5: Model response under isothermal tension-compression loads based on parementers of Tab. 2

Plastic behavior is now in focus considering bigger stresses than the yield limit. For the parameters from the Tab. 2, the figure (6) compares the material's PE and SM responses after accumulation of plastic strain. The forward transformation threshold reduction makes clear the model has coupled phase transformation and plasticity inelasticities. It indicates his suitability for TWSME training. Comparing SM and PE curves leads to the conclusion that all residual transformation strain can be removed by a thermal treatment, but the plastic strain keeps unchanged, establishing a new origin for stress free material in SM regime, which is equal to that in the PE one.

5. CONCLUSIONS

This paper presents a novel one-dimensional constitutive model to describe the thermomechanical behavior of shape memory alloys. The model is developed withing the framework of continuum mechanics and the generalized standard materials. Four macroscopic phases are considered. Classical plasticity with kinematic and isotropic hardening are treated. The main idea is to define inelastic surfaces that represent all irreversible process associated with both phase transformation and plasticity. Numerical simulations are carried out promoting a model verification compared with experimental data. Afterward, some classical tests are performed showing the model capabilities. In general, the model captures the general behavior of SMAs presenting nonparallel phase transformation surfaces and tension-compression asymmetry.

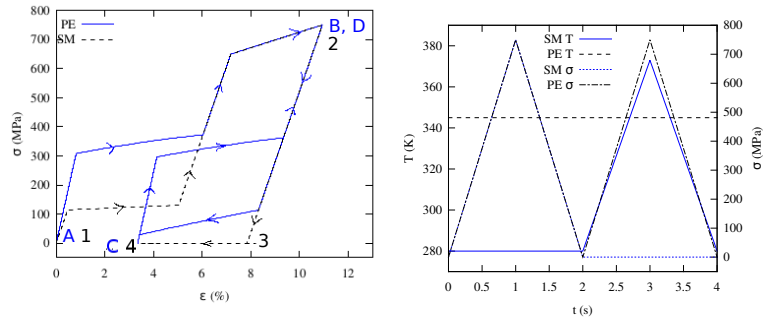

(a) Plastic responses under PE and SM regimes

(b) Loads applied for plastic simulation

Figure 6: Plastic behavior of SMAs PE (345 K) and SM regimes (280 K + thermal cycle)

6. ACKNOWLEDGEMENTS

The authors would like to acknowledge the support of the Brazilian Research Agencies CNPq, CAPES and FAPERJ and through the INCT-EIE (National Institute of Science and Technology - Smart Structures in Engineering) the CNPq and FAPEMIG. The Air Force Office of Scientific Research (AFOSR) is also acknowledged.

7. REFERENCES

Auricchio, F., Taylor, R.L. and Lubliner, J., 1997. "Shape-memory alloys: macromodelling and numerical simulations of the superelastic behavior". *Computer Methods in Applied Mechanics and Engineering*, Vol. 146, No. 3-4, pp. 281 – 312. ISSN 0045-7825. doi:http://dx.doi.org/10.1016/S0045-7825(96)01232-7. URL `http://www.sciencedirect.com/science/article/pii/S0045782596012327`.

Bo, Z. and Lagoudas, D.C., 1999. "Thermomechanical modeling of policrystalline smas under cyclic loading". *International Journal of Engineering Science*, Vol. 37, pp. 1089–1249.

de Souza, A.C.C., 1998. *Um modelo constitutivo tridimensional para ligas memória de forma*. Tese de D.Sc., COPPE/UFRJ, Rio de Janeiro, RJ, Brasil.

Lagoudas, D., 2008. *Shape Memory Alloys: Modeling and Engineering Applications*. Springer ebook collection / Chemistry and Materials Science 2005-2008. Springer, United States of America. ISBN 9780387476858.

Paiva, A., Savi, M.A., Braga, A.M.B. and Pacheco, P.M.C.L., 2005. "A constitutive model for shape memory alloys considering tensile-compressive asymmetry and plasticity". *International Journal of Solid and Structures*, Vol. 42, pp. 3439–3457.

Paiva, A. and Savi, M.A., 2006. "An overview of constitutive models for shape memory alloys". *Mathematical Problems in Engineering*, Vol. 2006, p. 30. doi:doi:10.1155/MPE/2006/56876. Article ID56876.

Rizzoni, R. and Marfia, S., 2015. "A thermodynamical formulation for the constitutive modeling of a shape memory alloy with two martensite phases". *Meccanica*, Vol. 50, No. 4, pp. 1121–1145. ISSN 0025-6455, 1572-9648. doi: 10.1007/s11012-014-0078-8. URL `http://link.springer.com/10.1007/s11012-014-0078-8`.

Savi, M.A., Paiva, A., Baeta-Neves, A.P. and Pacheco, P.M., 2002. "Phenomenological modeling and numerical simulation of shape memory alloys: a thermo-plastic-phase transformation coupled model". *Journal of Intelligent Material Systems and Structures*, Vol. 13, No. 5, pp. 261–273.

Tobushi, H., Iwanaga, H., Tanaka, K., Hori, T. and Sawada, T., 1991. "Deformation behaviour of tini shape memory alloy subjected to variable stress and temperature". *Continuum Mechanics and Thermodynamics*, Vol. 3, No. 2, pp. 79–93. ISSN 0935-1175. doi:10.1007/BF01129028. URL `http://dx.doi.org/10.1007/BF01129028`.

8. RESPONSIBILITY NOTICE

The following text, properly adapted to the number of authors, must be included in the last section of the paper: The author(s) is (are) the only responsible for the printed material included in this paper.